

A climatic atlas of the air-sea interaction parameters and fluxes of the oceans using satellite data

M.R. Ramesh Kumar^{1,2}, J. Schulz² and V. Jost³

¹National Institute of Oceanography, Dona Paula, Goa - 403 004, India.

²German Aerospace Centre, Cologne, Germany.

³Meteorological Institute, University of Hamburg, Germany.

186

Abstract

The present climatic atlas is based on the newly available data set known as the Hamburg Ocean Atmosphere Parameters and fluxes from Satellite data (HOAPS), for the global oceans. It presents the basic fields of air-sea interaction parameters such as sea surface temperature, specific humidity at air and sea surface temperature, difference in humidity, transfer coefficients, wind speed and the air sea fluxes such as latent heat, sensible heat and longwave radiation. The atlas also provides the hydrological cycle parameters over the global oceans such as evaporation, precipitation and freshwater flux. The data set covers the period July 1987 to December 1998 and provides the mean monthly, seasonal and annual fields of different variables. It is intended to provide a climatological data base for scientists in the field of climatology and air-sea interaction. We hope that this atlas will serve as a reference to the students as well as the scientists working in the fields of Climatology, Meteorology and Oceanography and also to others who are engaged in these fields.

1. Introduction

Oceans play a very important role in the global climate. It absorbs the most of the incoming shortwave solar radiation entering the earth atmosphere system and then redistributes with the oceanic environment by both horizontal and vertical oceanic movements. This energy is then further transported back into the atmosphere in the form of air-sea fluxes such as latent and sensible heat fluxes and longwave radiation flux, which are the main sources of energy for the atmospheric circulation. The tropical oceans are the regions of net radiation gain. This excess energy is transported into the higher latitudes by the atmosphere and the oceans to maintain the energy balance. Further, the tropical oceans are the regions where active air-sea interaction processes such as Monsoons and El Nino and Southern Oscillations takes place. Thus the study of air-sea interaction parameters, fluxes and the hydrological cycle of the global oceans are quite important for our understanding the climate variation.

In the past, several authors have made important contributions in the form of atlases mostly using the ship data (Baumgartner and Reichel, 1975; Hastenrath and Lamb, 1977, 1978, 1979; Ismer and Hasse, 1987; Oberhuber, 1988; da Silva et al., 1994; Josey et al., 1996). All the above studies have provided useful information on the various aspects of air-sea interaction parameters and fluxes. But the major drawback of most of these studies has been scarcity of the data over the data sparse regions such as Indian Ocean and southern

Oceans. Typically the satellite data has a much better spatial as well as temporal resolution than the ship data which is quite important for computing the monthly means..

Of the three major oceans, the Pacific Ocean has the largest range in the east-west extent of 140° longitude. On the western part of the Pacific Ocean, there exists one of the warmest regions in the world, the so called warmpool, in the eastern equatorial Pacific, there exists a well developed cold tongue. This large thermal gradient and the corresponding atmospheric circulation over this region has profound influence on the weather and climate over several parts of the world.

In this atlas we are presenting the monthly mean of 1° latitude and longitude resolution in addition to the seasonal and annual means. The seasonal means of Winter, Spring, Summer and Fall are representative of the mean of December, January and February; March, April and May; June, July and August and September, October and November respectively.

2. Data and methodology

The evaporation at the sea surface is parameterised using the bulk approach. The wind speed u , the saturation specific humidity at the sea surface (q_s) and specific humidity at air temperature (q_a) are determined from satellite measurements. Wind speed is retrieved following Schuessel and Luthardt (1991) which

determines the wind speed at 10 m mainly from the brightness temperature difference between horizontally and vertically polarised components at frequencies of 19 and 37 GHz of the SSMI data. Intercomparison to buoy and ship measurements revealed an rms mean square error of approximately 2 m s^{-1} with no bias. The most difficult parameter to retrieve is the specific humidity of air, q_a . Liu (1986) was the first to retrieve the atmospheric humidity from total precipitable water from the atmosphere. Schulz et al. (1993) were able to retrieve the integrated water vapour content in the lowest 500 m of the atmosphere and this parameter was found to correlate well ($r > 0.9$) and linearly with the specific humidity near the ocean's surface. The recent method of Schluessel (1996) has further refined the technique of Schulz et al. (1993) concerning some biases in the polar basins.

We have used the NOAA/NASA Pathfinder Sea Surface Temperature product for the computation of specific humidity at the sea surface, q_s . These SST's are available as daily fields with a spatial resolution of 9 km. The daily fields of SST are combined with the instantaneous retrievals of wind speed and specific humidity on a rectangular grid.

In the present study, we use the algorithm developed by Bauer and Schluessel (1993) for the rainfall estimate. This algorithm has been successfully tested within the Precipitation Intercomparison Project (PIP) and Algorithm Intercomparison Project (AIP).

Lastly, we have incorporated some empirical assumptions in the computations. The most important one being that of atmospheric stability to compute the transfer coefficient. Within the scheme of Smith (1988) it is assumed that the atmosphere has a relative humidity of 80% at any given time. With the above assumption,

the air temperature can be computed from the estimated q_a . The errors in the transfer coefficient that can occur if this assumption is wrong are between 2% at high wind speeds and strong unstable conditions to 50% at low wind speeds and strong stable conditions (Schulz et al., 1997). Fortunately, areas with a stable temperature stratification are not very large and do not occur too often, so that the described errors in the transfer coefficients does not affect the monthly and annual time averages over the Ocean basins.

Section 2 describes the basic state variables such as sea surface temperature (SST); specific humidity at SST (q_s); surface air specific humidity(q_a); difference in humidity; transfer coefficients and wind speed. In section 3, the air-sea fluxes such as latent and sensible heat fluxes and long wave radiation flux are presented. Section 4 describes the hydrological cycle parameters such as evaporation, rainfall and fresh water flux. A brief summary is presented in Section 5.

2. Basic state variables

2.1. Sea surface temperature

The most important feature of the SST distribution is the large east-west gradient in the Pacific Ocean. Another important feature is the summer monsoonal cooling in the Arabian Sea, whereas the rest of the northern oceans exhibit warmer SST's. Further there exists a warm pool region in the western Pacific and eastern Indian Ocean during most part of the year. The southern Indian Ocean region experiences very little annual variation and remains cool throughout the year. The north Indian Ocean and the Arabian Sea in particular undergoes dramatic variations with onset of summer monsoon. With the development of the strong cross equatorial flow, relatively cooler waters appear along

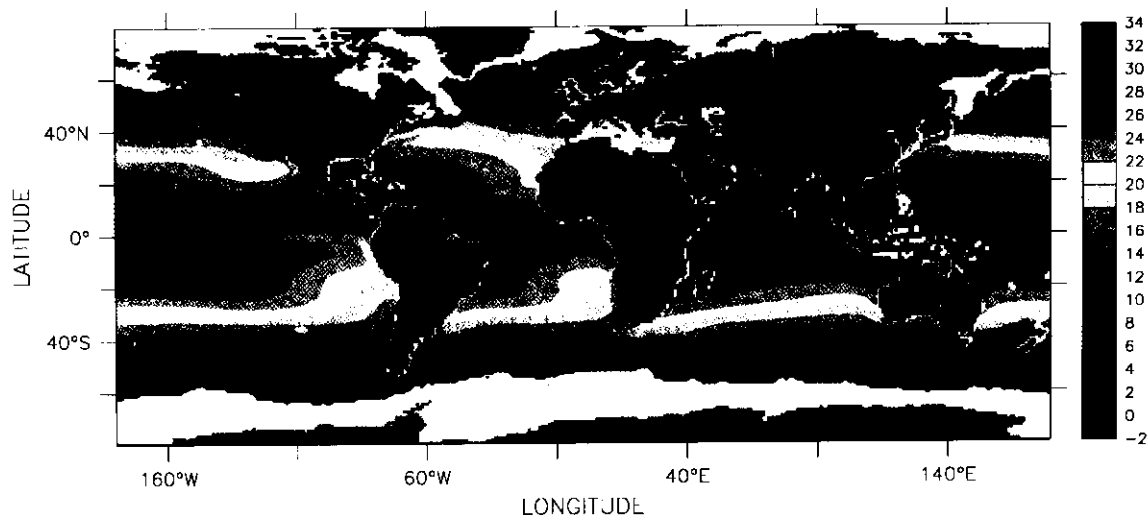


Fig. 1. Mean annual distribution of sea surface temperature over the oceans ($^{\circ}\text{C}$).

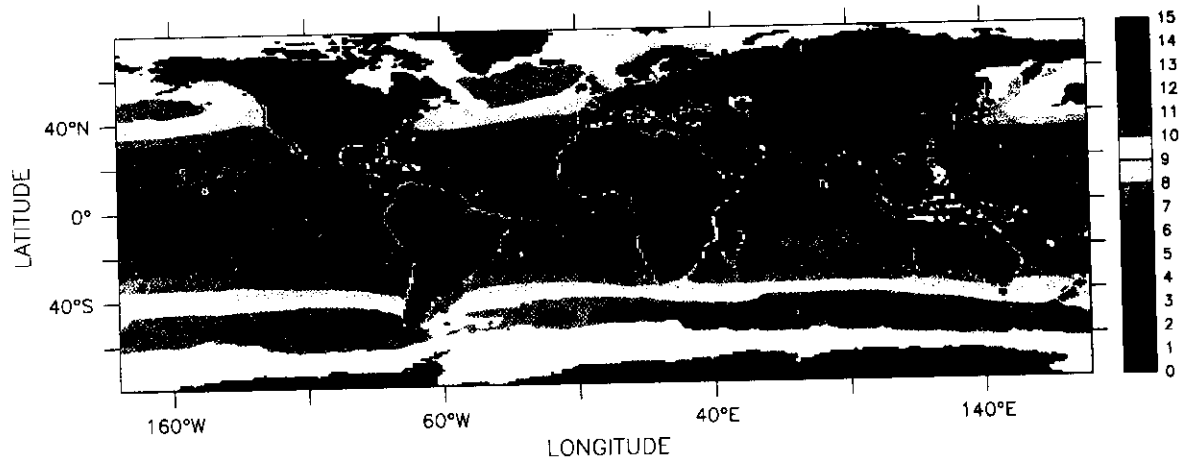


Fig. 2. Mean annual distribution of wind speed over the oceans (m/sec).

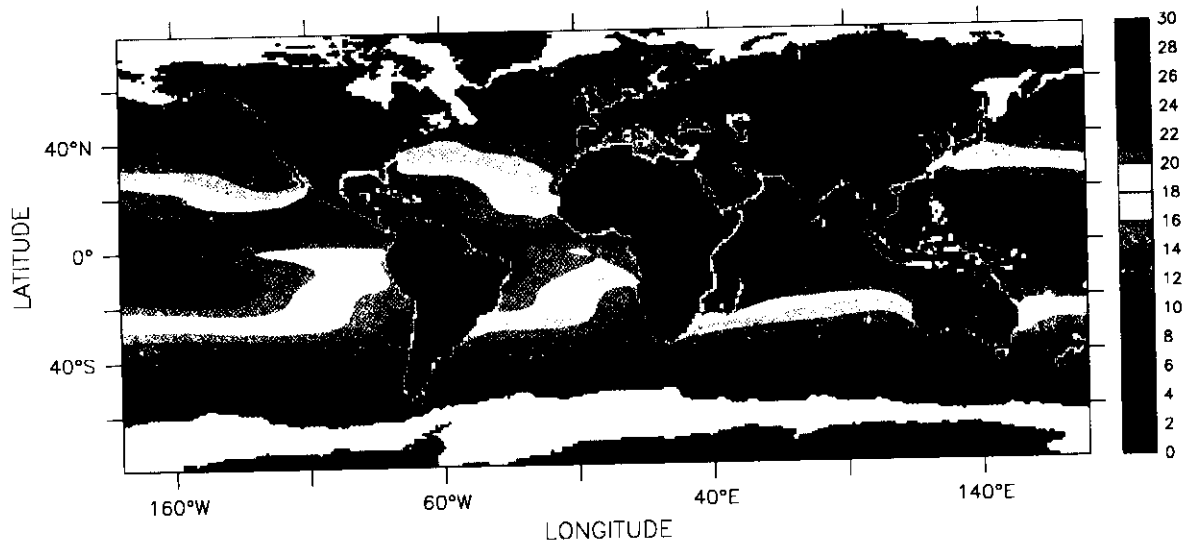


Fig. 3. Mean annual distribution of specific humidity at sea surface temperature over the oceans (g/kg).

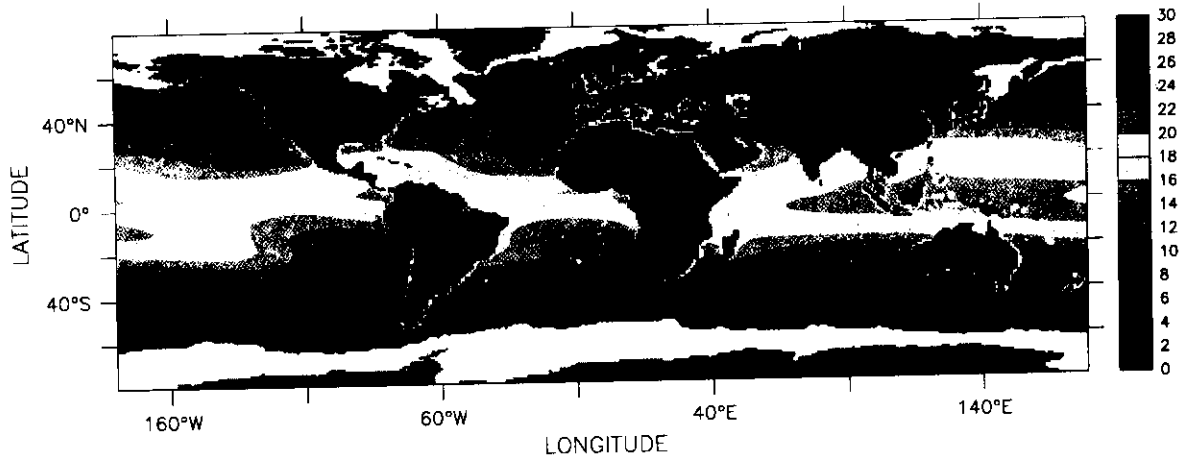


Fig. 4. Mean annual distribution of specific humidity at air temperature over the oceans (g/kg).

the coasts of Somalia and Arabia due to the upwelling processes. The meridional SST gradient is strong in the north Pacific Ocean during the winter as compared to the summer when it is quite weak. Fig. 1 presents the mean annual SST distribution over the oceans.

The most important features are the warm pool region in the central and eastern equatorial Indian Ocean region, western and central Pacific Ocean. The cold tongue of SST spreads from the south American continent to the central Pacific region.

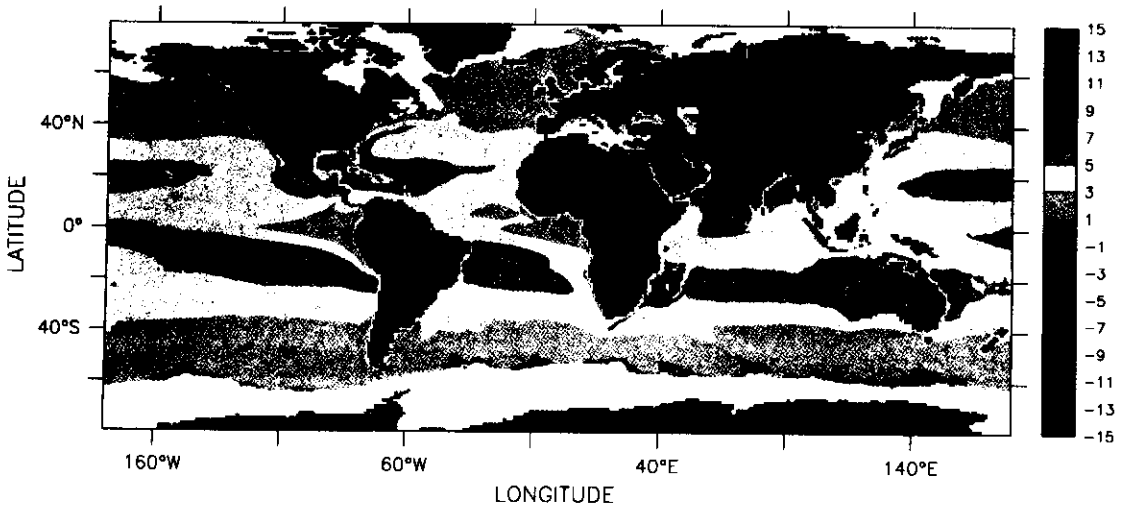


Fig. 5. Mean annual distribution of difference in humidity over the oceans (g/kg).

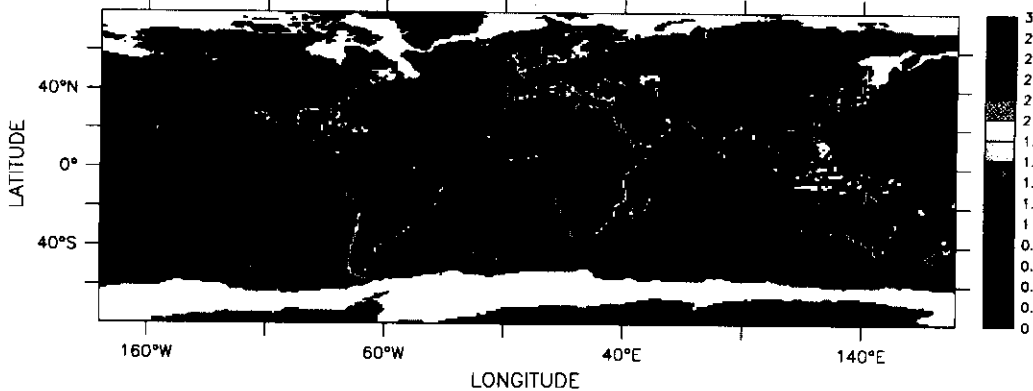


Fig. 6. Mean annual distribution of transfer coefficients over the oceans.

2.2. Wind speed

The maximum wind speeds (>12 m/s) are observed over the north Atlantic Ocean during the winter months and they gradually decrease in their intensity in the spring. In the winter months, the minimum wind speeds are found in the north Indian Ocean, both in the Arabian Sea and Bay of Bengal. With the onset of summer monsoon, i.e. from June till September, a strong cross equatorial flow develops over the western equatorial Indian Ocean, which bring along with it copious amount of moisture into Arabian Sea and Indian subcontinent. Another region of large wind speeds throughout the year are the sub-tropical southerlies whose wind speed exceeds 10 m/s (Fig. 2).

2.3. Specific humidity at sea surface temperature (q_s)

The specific humidity at SST figures are quite similar to the SST charts as they have the maximum influence. The maximum q_s values can be expected in the warm pool regions of the eastern Indian and western Pacific Oceans and the lowest values are found in the regions

where SST's are quite low. On a seasonal scale, the maximum values are to be found in spring, summer and fall seasons as compared to the winter season. The largest q_s values are to be found in the north Atlantic Ocean during the summer and fall seasons especially in the Gulf of Mexico. The largest values of q_s (> 22 g/kg) are observed over the warm pool regions and the lowest (<10 g/kg) over the polar regions (Fig. 3).

2.4 Specific humidity at air temperature (q_a)

The distribution of q_a is dependent on the surface air temperature and to a certain extent follows the SST pattern. The highest values are observed in the warm pool region, i.e., the eastern Indian Ocean and western Pacific Ocean. The maximum q_a values are observed in the Bay of Bengal and the adjacent south China Sea (>20 g/kg) during the monsoon season, even though areal extent of the warm pool region is much more larger. The mean annual distribution of q_a (Fig. 4) shows that the maximum values (> 20 g/kg) are observed over a very narrow strip as compared to the q_s distribution.

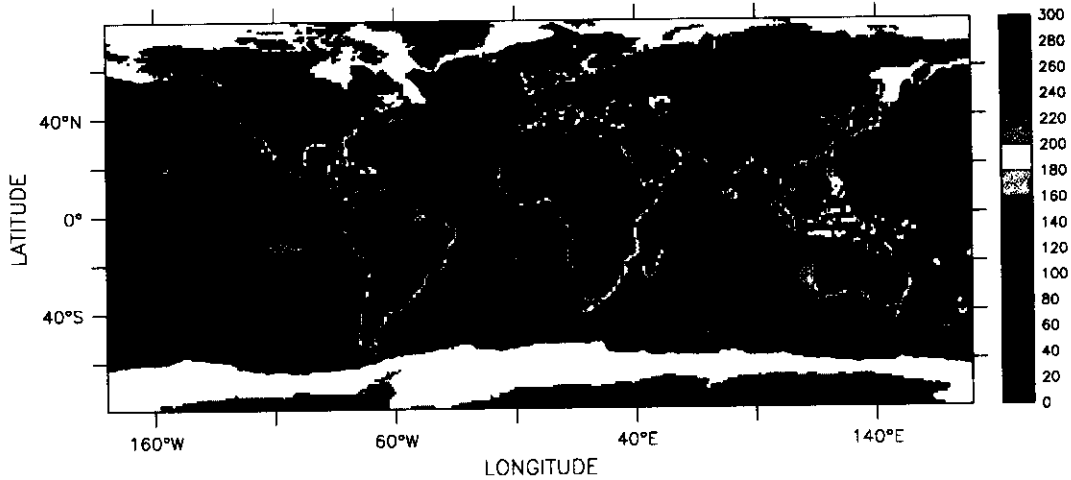


Fig. 7. Mean annual distribution of latent heat flux over the oceans (W/m^2).

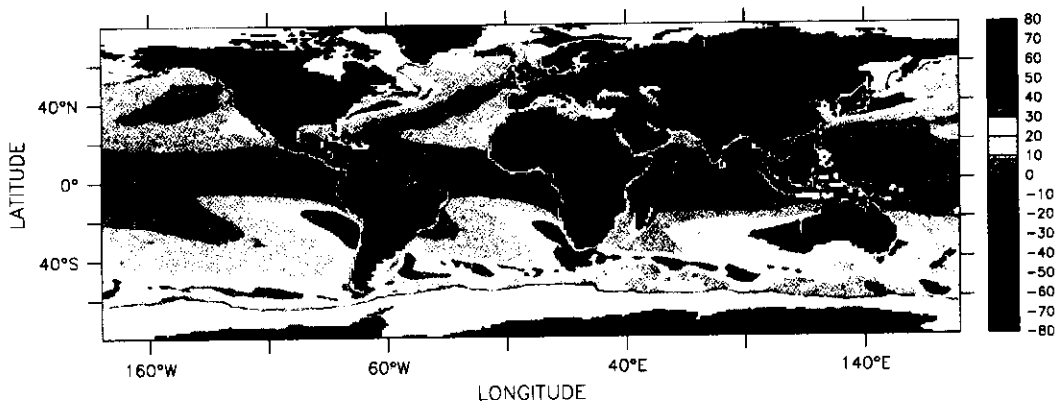


Fig. 8. Mean annual distribution of sensible heat flux over the oceans (W/m^2).

2.5 Difference in humidity

The distribution of difference in humidity shows that the maximum differences are seen in the north Indian Ocean, i.e., in the Arabian Sea and Bay of Bengal during the winter months, (December, January and February). On an annual scale also the Persian Gulf, Red Sea and the northern Arabian Sea are the regions of the largest difference in humidity (Fig. 5).

2.6 Transfer or exchange coefficients

The transfer or the exchange coefficients are very important for computing the latent heat flux as well as the evaporation. They are dependent upon the atmospheric stability and wind speed. The lowest values are observed in eastern equatorial Pacific and Atlantic Oceans throughout the year and highest values are observed in the northern Arabian Sea during the winter, spring and fall seasons. On annual scale (Fig 6) large transfer coefficients are observed over the northern Arabian Sea and off the west Australian coasts.

3. Air-sea fluxes

The surface heat budget of the oceans is an integral part general circulation of the atmosphere. The heat-

ing of the atmosphere largely occurs by the transfer of fluxes of sensible and latent heat from the oceans to the atmosphere in the tropical regions. The longwave radiational flux also plays an equally important role. In this section, we present the latent and sensible heat fluxes as well as the longwave net radiation.

3.1 Latent heat flux (LHF)

The latent heat flux is the major source of energy for the atmosphere. The latent heat flux is a function of wind speed, difference in humidity and the atmospheric stability. The regions of maximum LHF values are seen in the Kuroshio and Gulf Stream regions during the winter months. The regions of the lowest LHF values are found in the eastern equatorial Pacific and Atlantic Oceans during the winter and spring. During summer season the minimum LHF values are observed in the northern parts of Atlantic and Pacific Oceans. During the fall season, the minimum is observed in south American and southwest African coast. On an annual scale (Fig. 7), the LHF values are higher in the south Indian Ocean as compared to the northern counter part and is the major source of moisture for the summer monsoon rainfall for the Indian subcontinent.

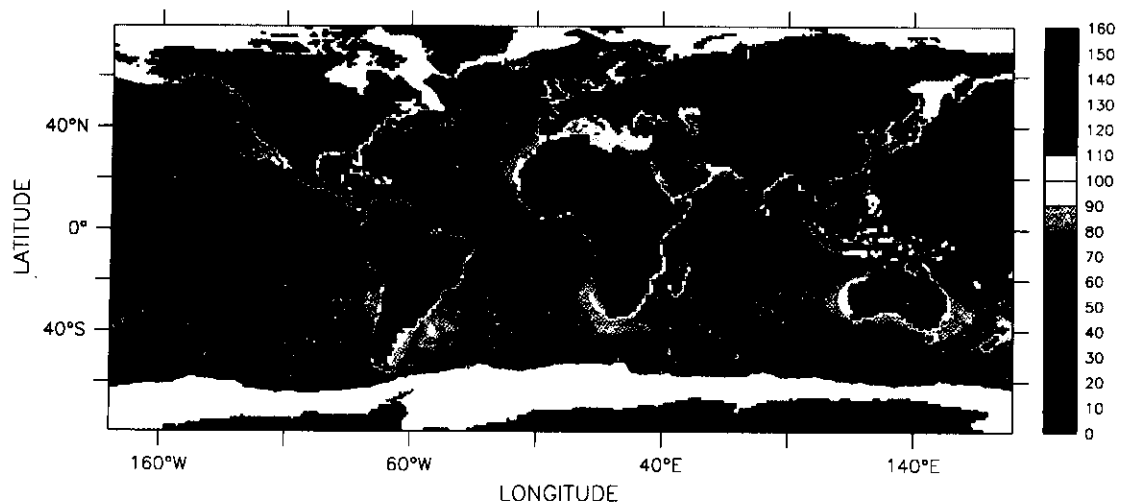


Fig. 9. Mean annual distribution of longwave radiation flux over the oceans (W/m^2).

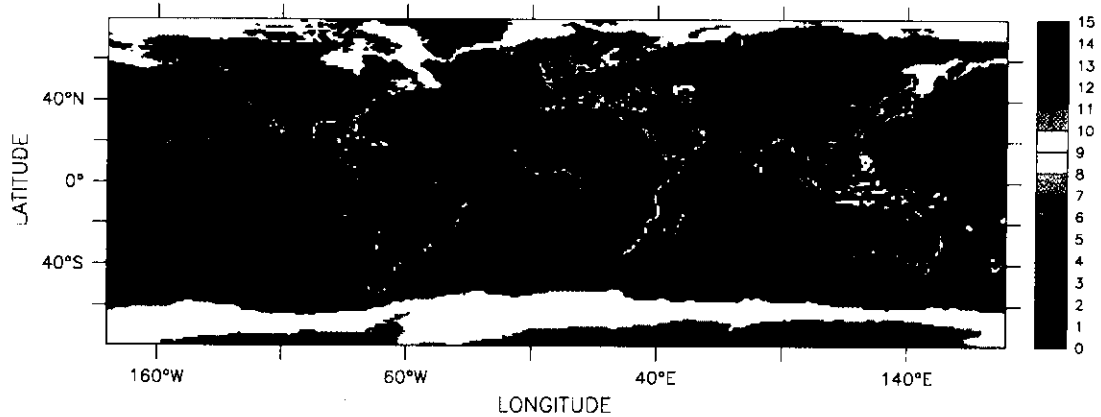


Fig. 10. Mean annual distribution of evaporation over the oceans (mm/day).

3.2 Sensible heat flux (SHF)

The sensible heat flux distribution to a certain extent broadly follows that of SST and the sea-air temperature difference. The SHF, unlike the LHF can be positive and negative as well. The positive values mean the flow from the ocean to the atmosphere and the negative values mean the flow from the atmosphere into the ocean. The negative values of SHF, in general, occur over the major upwelling zones of the global oceans. During the winter season, we observe large areas of positive SHF off the eastern parts of the continents, as the cold dry air from the continents flows over the warm currents of Kuroshio and Gulf Stream from November till March and this then disappears in April. During the summer season, the maximum values are observed in the southern oceans, especially in the south Indian Ocean. During the summer period, the entire north Indian ocean loses heat to the atmosphere, with region off Somalia coast experiencing the maximum heat loss (-20 to $-40 Wm^{-2}$). The mean annual picture (Fig. 8) shows the Kuroshio, Gulf Stream and the region off the western Australian coast and south Africa as having large positive SHF values.

3.3 Longwave net radiation (LWR)

The longwave net radiation is another important energy source for the atmosphere after the LHF flux. It is dependent upon the sea surface temperature and surface air humidity. The low values occur usually over the cloudy regions such as the Inter Tropical Convergence Zones (ITCZ's). This dramatic variation in the LWR can be clearly seen in the Arabian Sea and Bay of Bengal, where the maximum values of $100-140 Wm^{-2}$ drops drastically with the progress of the ITCZ into the north Indian Ocean by $0-40 Wm^{-2}$ in the monsoon months when the ITCZ merges with the monsoon trough over the Indian subcontinent. The LWR then gradually increases with the withdrawal of the summer monsoon (i.e., from October to January). On an annual scale (Fig. 9), the lowest values are observed in the southern Pacific and Atlantic Oceans just south off the equator.

4. Hydrological cycle

The hydrological cycle parameters, namely, evaporation, precipitation and fresh water flux show significant variations both on monthly and seasonal scale.

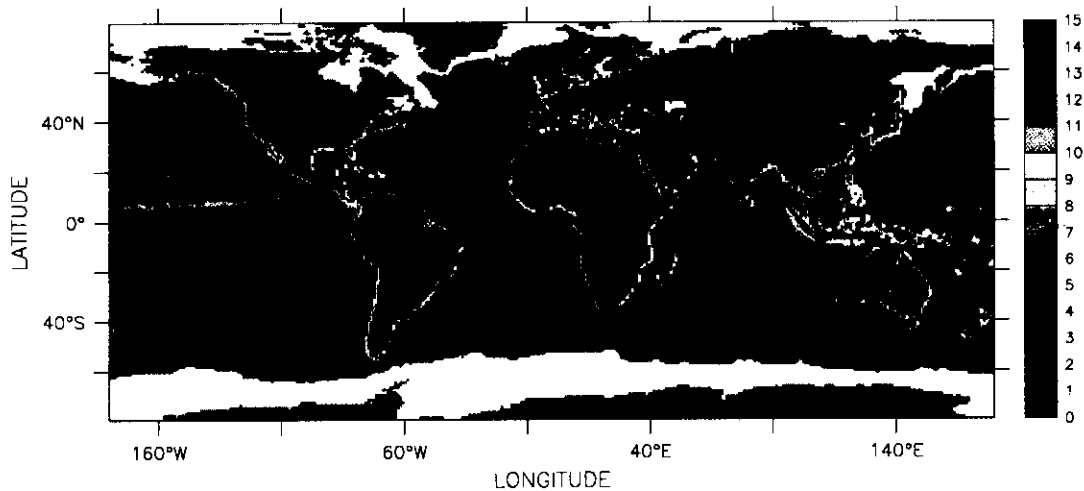


Fig. 11. Mean annual distribution of precipitation over the oceans (mm/day).

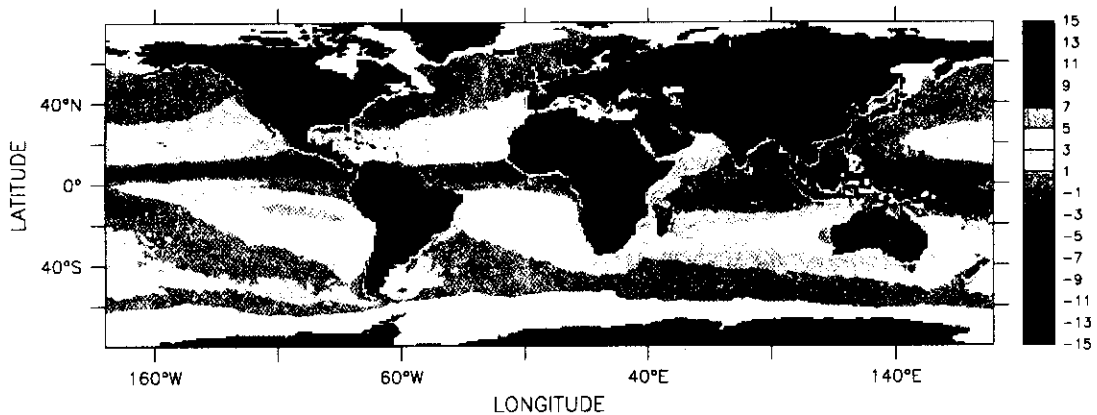


Fig. 12. Mean annual distribution of fresh water flux over the oceans (mm/day).

4.1 Evaporation (E)

The evaporation maps are very similar to the LHF maps with the maximum values observed over the Kuroshio (> 9 mm/day) and Gulf Stream regions in winter and the minimum values (< 1 mm/day) seen in the eastern equatorial Pacific and Atlantic Oceans. In the case of the summer, the maximum values are observed in the south Indian, Atlantic and Pacific Oceans. The mean annual cycle of evaporation (Fig. 10) shows the maximum values in the southern oceans, in addition, we observe high values in the Kuroshio and Gulf Stream. The lowest values are observed in the eastern equatorial Pacific and Atlantic Oceans.

4.2 Precipitation (P)

The maximum precipitation occurs over the ITCZ regions where P exceeds more than 6 mm/day. The other notable regions where large scale precipitation occurs is over the Gulf Stream and Kuroshio region during the period November to March. With the onset of summer monsoon, the ITCZ, which was in the south

Indian Ocean traverses to its northern most extent and merges with the Monsoon Trough giving rise to copious amount rainfall over the Indian subcontinent and the adjoining sea areas, namely the Arabian Sea and Bay of Bengal. On annual scale (Fig. 11) it can be seen that the region off the Indonesian islands receive the maximum rainfall of more than 10 mm/day. The other regions receiving substantial rainfall are the Kuroshio region, Gulf Stream and north Pacific Convergence Zone.

4.3 Fresh water flux

The fresh water flux, which we have computed as the difference of evaporation and precipitation shows that $E - P$ is negative over the regions where rainfall is maximum and these are the Intertropical Convergence Zone areas. The other regions where $E - P$ is negative is over the Gulf Stream and Kuroshio region. An analysis of the fresh water flux on a seasonal scale, shows that the eastern parts of the Arabian Sea, Bay of Bengal and south China Sea all have negative values of fresh wa-

ter flux during the summer and fall seasons. Further, on an annual scale (Fig. 12), it can be seen that eastern equatorial Indian Ocean, Bay of Bengal, Kuroshio and the Gulf Stream regions all exhibit negative fluxes. The regions of positive flux are over the northwest Arabian Sea and south Indian Ocean south of 20°S. Also the north Atlantic and south Atlantic regions on both sides of the ITCZ also exhibit positive fluxes.

5. Summary and Conclusions

This atlas for the first time presents the various air-sea interaction parameters such as sea surface temperature, specific humidity at sea surface and air temperatures, difference in humidity, transfer coefficients and wind speed; air-sea fluxes such as latent and sensible heat fluxes and longwave net radiational flux and the hydrological cycle parameters such as evaporation, precipitation and fresh water flux on a much better spatial and temporal resolution as compared to the conventional in-situ or ship measurements. Further, the satellite measurements are well distributed in both in space and time which are quite important for giving a meaningful monthly mean as compared to the traditional ship observations. This atlas, we hope will be quite useful as a reference material for the students as well as the research scientists who are working in the fields of Climatology, Meteorology and Oceanography and those engaged in similar activities.

Acknowledgements

This work forms part of the Indo-German Collaborative Programme on Air-Sea Interaction which is funded by the International Office of the German Ministry of Education, Research and Technology (BMBF). This support is gratefully acknowledged. M.R. Ramesh Kumar thanks Prof. C. Simmer, Head, Meteorological Institute, University of Bonn, for providing the Library facilities of that Institute. All the plots and graphs were drawn with the Ferret Software, provided by NOAA/PMEL, USA. M.R.R.K. was supported by a DST grant. This is NIO contribution No. 3587.

References

- Bauer, P., and P. Schluessel, 1993: Rainfall, total water, ice water, and water vapour over sea from polarized microwave simulations and Special Sensor Microwave /Imager data. *J. Geophys. Res.*, 98, 20737-20759.
- Baumgartner, A., and E. Reichel, 1975: *The World Water Balance: Mean Annual Global, Continental and Maritime Precipitation, Evaporation and Runoff*, Elsevier, 179 pp.
- Da Silva, A., C. C. Young and S. Levitus, 1994: *Atlas of Surface Marine Data 1994 Vol. 1. Algorithms and Procedures*. NOAA Atlas NESDIS 6, U.S. Dept. of Commerce, Washington, D.C., 83 pp.
- Hastenrath, S., and P.J. Lamb, 1977: *Climatic Atlas of the Tropical Atlantic and Eastern Pacific Oceans*, University of Wisconsin Press, Madison, 340 pp.
- Hastenrath, S., and P.J. Lamb, 1978: *Heat Budget Atlas of the Tropical Atlantic and Eastern Pacific Oceans*, University of Wisconsin Press, Madison, 104 pp.
- Hastenrath, S., and P.J. Lamb, 1979: *Climatic Atlas of the Indian Ocean, Part I: Surface Circulation and Climate*. University of Wisconsin Press, Madison, USA.
- Hastenrath, S., and P.J. Lamb, 1979: *Climatic Atlas of the Indian Ocean, Part II: The Oceanic heat budget*, University of Wisconsin Press, Madison, USA.
- Liu, W.T., 1986: Statistical relation between monthly mean precipitable water and surface level humidity over global oceans. *Mon. Wea. Rev.*, 114, 1591-1602.
- Oberhuber, J. M., 1988: An Atlas based on the COADS Data Set: The budgets of Heat, Buoyancy and Turbulent Kinetic Energy at the surface of the Global Ocean. Max-Planck-Institut für Meteorologie, Rep.No.15.
- Schluessel, P., 1996: *Satellite remote sensing of evaporation over sea. Radiation and water in climate system: Remote measurements*, edited by Erhard Raschke, NATO ASI Series, Vol.145, Springer and Verlag, Heidelberg, 431-461.
- Schluessel, P., and H. Luthardt, 1991: Surface wind speeds over the North Sea from Special Sensor Microwave/Imager observations. *J. Geophys. Res.*, 96, 4845-4853.
- Schulz, J., P.Schluessel and H. Grassl, 1993: Water Vapour in the atmospheric boundary layer over oceans from SSM/I measurements. *Int. J. Remote Sensing*, 14, 2773-2789.
- Schulz, J., J. Meywerk, S. Ewald and P. Schluessel, 1997: Evaluation of satellite derived latent heat fluxes. *J. Climate*, 10, 2782-2795.
- Schulz, J., V. Jost and S. Bakan., 1998: A New satellite derived freshwater climatology (Hamburg Ocean Atmosphere Parameters and Fluxes from Satellite Data). *International WOCE Newsletter*, 32, 20-26.
- Smith, S.D. (1988): Coefficients for sea surface wind stress, heat flux, and wind profiles as a function of wind speed and temperature. *J. Geophys. Res.*, 93, 2859-2874.